

Analyzing Change in Yellowstone's Terrestrial Emittance with Landsat Imagery

Shannon L. Savage and Rick L. Lawrence¹

*Department of Land Resources and Environmental Sciences,
Montana State University, Bozeman, Montana 59717*

Stephan G. Custer

*Department of Earth Sciences,
Montana State University, Bozeman, Montana 59717*

Jeffrey T. Jewett and Scott L. Powell

*Department of Land Resources and Environmental Sciences,
Montana State University, Bozeman, Montana 59717*

Joseph A. Shaw

*Department of Electrical and Computer Engineering,
Montana State University, Bozeman, Montana 59717*

Abstract: Yellowstone National Park (YNP) contains the world's largest concentration of geothermal features and is legally mandated to protect and monitor these natural features. Remote sensing is a component of the current geothermal monitoring plan. Landsat satellite data have a substantial historical archive and will continue to be collected into the future, making it the only available thermal imagery for historical analysis and long-term monitoring of geothermal areas in the entirety of YNP. Landsat imagery from Thematic Mapper (TM) and Enhanced Thematic Mapper Plus (ETM+) sensors was used to examine change trajectories for terrestrial emittance among spatial groupings from 1986 to 2007. Trajectories of locations with known change events were also examined. Relationships between the spatial groupings and several change vectors (distance to geologic faults, distance to large water bodies, and distance to earthquake swarms) were explored. The analysis showed the strongest relationship between absolute difference in terrestrial emittance and earthquake swarms, with 34% of the variation explained. Certain known change events were reflected in the change trajectories, while the Landsat imagery was not able to detect other known events. This suggests that Landsat imagery might be a useful tool for monitoring geothermal responses in YNP, but cannot be expected to suffice as the sole monitoring tool.

INTRODUCTION

Geothermal features are one of the main reasons that Yellowstone National Park (YNP) was established as the world's first national park. YNP contains the greatest

¹Corresponding author: email: rickl@exchange.montana.edu

concentration of geothermal features in the world (Waring et al., 1983) and is listed as a significant geothermal feature itself (Geothermal Steam Act, 1970 as amended in 1988). The National Park Service (NPS) is legally mandated to monitor and protect geothermal features within its units.

Geothermal heat flux (GHF), measured in watts per meter squared (Wm^{-2}), is the driver of the dynamics of geothermal features. The GHF in the Yellowstone region is approximately 2 Wm^{-2} , which is roughly 40 times the world continental heat flow of 0.04 to 0.06 Wm^{-2} (Smith and Siegel, 2000; University of Utah, 2011). GHF is heat change in water and steam in geothermal systems that is radiated from the surface of the Earth and can be remotely sensed from satellites (Savage et al., 2010). GHF represents only heat coming from below the surface and does not include accumulated indirect or direct solar heating effects, such as convection from air currents and soil conduction of solar effects (indirect), or solar heating due to variations in topography (direct). In contrast, terrestrial emittance (M_{terr}) represents all heat emitted from the ground and is composed of GHF as well as direct and indirect solar radiation effects. Attempts have been made to account for solar effects relative to M_{terr} at a YNP-wide scale with some success, but also with some limitations (Savage et al., 2010). Change analysis within specific geothermal areas, however, requires data with low variability for unchanged features at local scales, allowing for the observation of actual change rather than data noise. Our previous study (Savage et al., 2010) revealed that M_{terr} has several advantages over estimates of GHF for analyzing change in YNP's geothermal areas. First, M_{terr} has been field verified (Watson et al., 2008), while GHF approaches have not due to logistical constraints. Second, the spatial patterns of GHF as estimated by current methods are substantially different from those of the less variable M_{terr} , including data striping artifacts and overly high values on north-facing slopes (Savage et al., 2010). Lastly, all things being equal, the level of uncertainty in the data increases with each additional processing step, and M_{terr} requires less processing than GHF.

Changes in M_{terr} can be used to examine changes in behavior of geothermal features or to monitor for changes in heat flux that might be occurring in response to land management practices within and outside of YNP. New features regularly emerge and active features become inactive. The geothermal features of YNP must be monitored on a regular basis to enable observers to assess changes that might occur over days or decades. Having multiple dates of M_{terr} readings would permit examination of patterns in M_{terr} change to try to relate them to possible factors that might cause change.

Ideas abound as to why geothermal features change, with seismic activity (both near and distant) being the most widely accepted hypothesis (Ingebritsen and Rojstaczer, 1996; Rojstaczer et al., 2003). Changes in geyser activity within YNP were observed shortly after the 2002 7.9 magnitude Denali fault earthquake in Alaska, 3100 km away (Husen et al., 2004). Local earthquake swarms were also associated with geothermal activity change. Earth movement near or within geothermal features might shake open vent blockages (Husen et al., 2004) or seal vents and fractures, thus changing geothermal activity (Fournier et al., 1991; Dobson et al., 2003). Changes in climate or season also might have an effect on geothermal features (White et al., 1988; Fournier et al., 1991; Hurwitz et al., 2008). Drought and changes in barometric pressure can change ground water levels (Hurwitz et al., 2008; Ingebritsen and Rojstaczer, 1996). Geothermal features are linked with subterranean ground water (White et al., 1988; Fournier, 1989; Bryan, 2008). Changes in GHF observed in Barrow, Alaska from 1971

to 1992 have been attributed to an increase in surface temperatures and decrease in soil moisture (Oechel et al., 1995). Pressure changes in response to changing glacial ice and changing lake levels have led to large hydrothermal explosions and changes in the hydrothermal flow system and GHF in Yellowstone (Muffler et al., 1971; Morgan et al., 2007). Relationships between geologic faults and geothermal activity have been observed outside the 640,000-year-old caldera boundary in YNP (Pierce and Morgan, 1992; Finn and Morgan, 2002). "Heavy breathing" (regular uplift and subsidence) of the 640,000-year-old caldera in YNP has been modeled over recent millennia and associated with hydrogeothermal activity (Pierce et al., 2007). Recognized external threats to the geothermal features of YNP include potential geothermal development in Idaho and Montana, and oil, gas, and groundwater development in Wyoming, Montana, and Idaho (Sorey, 1991; Custer et al., 1993; Heasler et al., 2004; Barrick, 2010).

Details of change within geothermal systems (i.e., large areas of GHF as opposed to individual features), however, are poorly known. Knowledge about system-wide change might provide scientific insight into patterns that would help advance the understanding of processes in important geothermal systems. A better understanding of these systems would help inform scientists when management activities (both inside and outside YNP) are affecting geothermal resources, would help with placement of visitor information, and would be an important planning tool for placing infrastructure in YNP. Finally, there is a growing demand for alternative energy in the United States, and the development of widespread geothermal energy is likely. The impact of geothermal energy development outside YNP on geothermal features inside YNP will become an increasingly important issue. A geothermal monitoring plan that combines remote sensing of geothermal features with the inventory, monitoring, and assessment of both groundwater and chloride flux has been proposed for YNP to address these issues (Heasler et al., 2004). Remote sensing is an important element of the plan because it is an excellent way to assess historic change and has great potential to provide methods for future monitoring.

Geothermal resources at YNP have been studied in several different ways in the past. Nearly 12,000 individual features in YNP have been catalogued since 1998 (Spatial Analysis Center, 2008). The next greatest concentration of geothermal features is estimated to be in Iceland (over 500) and New Zealand (nearly 70; Waring et al., 1983). Rick Hutchinson, geologist for YNP from 1976 to 1996, spent many years studying the geothermal areas in YNP and during that time produced maps of geothermal area boundaries. Those maps have subsequently been updated and checked for accuracy by staff at YNP's Spatial Analysis Center to produce the most up-to-date digital map of defined geothermal areas (Spatial Analysis Center, 2005). Finally, chloride flux has been used as a proxy to determine convective heat flow in various regions of YNP (Fournier et al., 1975; Norton and Friedman, 1985; Friedman and Norton, 2007).

Several studies have used airborne multispectral digital imagery to evaluate geothermal features in the Norris Geyser Basin area (Hardy, 2005; Seielstad and Queen, 2009) and Upper and Midway Geyser Basins areas (Neale, 2008). A method of quantifying the intensity of surficial geothermal activity in YNP was developed with 2004 Landsat imagery and has good potential for geothermal monitoring (Watson et al., 2008). This method has been further refined and evaluated relative to GHF and M_{terr} calculations (Savage et al., 2010).

Landsat satellite imagery has been used successfully to perform many types of change analyses, making it a reasonable tool for monitoring M_{terr} at YNP over time. The short-wave infrared (SWIR) bands from the Landsat Thematic Mapper (TM) sensor were used to distinguish high-temperature fumarole vents and active lava bodies at Momotombo volcano in Nicaragua from 1989 to 1990 and Vulcano volcano in Italy from 1988 to 1989 (Oppenheimer et al., 1993). GHF was used to detect lava flowing in tubes at Kilauea volcano in July and October of 1991 utilizing TM data and laboratory measurements (Harris et al., 1998).

Some recent studies have successfully analyzed change trends over multiple years, although most methods of change detection make comparisons of only two dates (Lu et al., 2003). Change curves were developed with Landsat TM data to analyze change in vegetation on Mount St. Helens for 15 years following its eruption on 18 May 1980 (Lawrence and Ripple, 1999). Forest disturbance was detected and labeled with a trajectory-based change detection analysis of an 18-date time series of Landsat Enhanced Thematic Mapper Plus (ETM+) and TM data in western Oregon (Kennedy et al., 2007). There are no known multi-date or trajectory-based studies of geothermal heat in YNP.

The two main purposes of this project were to: (1) calculate M_{terr} in the defined geothermal areas of YNP for a time series spanning two decades; and (2) assess the changes in spatial distribution of M_{terr} in YNP's defined geothermal areas for that period. The value in this study lies in the near-annual observations of M_{terr} over multiple decades, covering all defined geothermal areas in YNP. The few studies done in YNP previously on this topic have been for a single date (Watson et al., 2008; Savage et al., 2010) and/or over limited geographic areas (Hardy, 2005; Seielstad and Queen, 2009).

METHODS

Study Area

YNP encompasses approximately 890,000 ha in Wyoming, Montana, and Idaho, USA (Fig. 1). Elevation ranges from 1567 m to 3458 m (Spatial Analysis Center, 1998). Vegetation includes grassland, shrubland, and forest, interspersed with bare ground. Average precipitation ranges from 25–30 cm in the lower elevations up to 203 cm in the higher elevations (Spatial Analysis Center, 2000), with warm, dry summers and cold, snowy winters (Western Regional Climate Center, 2005). The currently defined geothermal areas, at 6343 ha, comprise less than 1% of the entire area of YNP (Fig. 1). More than 60% of the defined geothermal areas are within the 640,000-year-old caldera boundary. Elevation in these areas ranges from 1728 m to 2775 m (Spatial Analysis Center, 1998). The majority of the vegetation within geothermal areas is grassland; however, shrubland, forest, and bare ground are also found. Average precipitation in the geothermal areas ranges from 35–203 cm (Spatial Analysis Center, 2000).

Data Acquisition

YNP is centered within one Landsat scene at Path 38, Row 29. Fourteen Landsat TM and Enhanced Thematic Mapper Plus (ETM+) summer images from 1986 to 2007

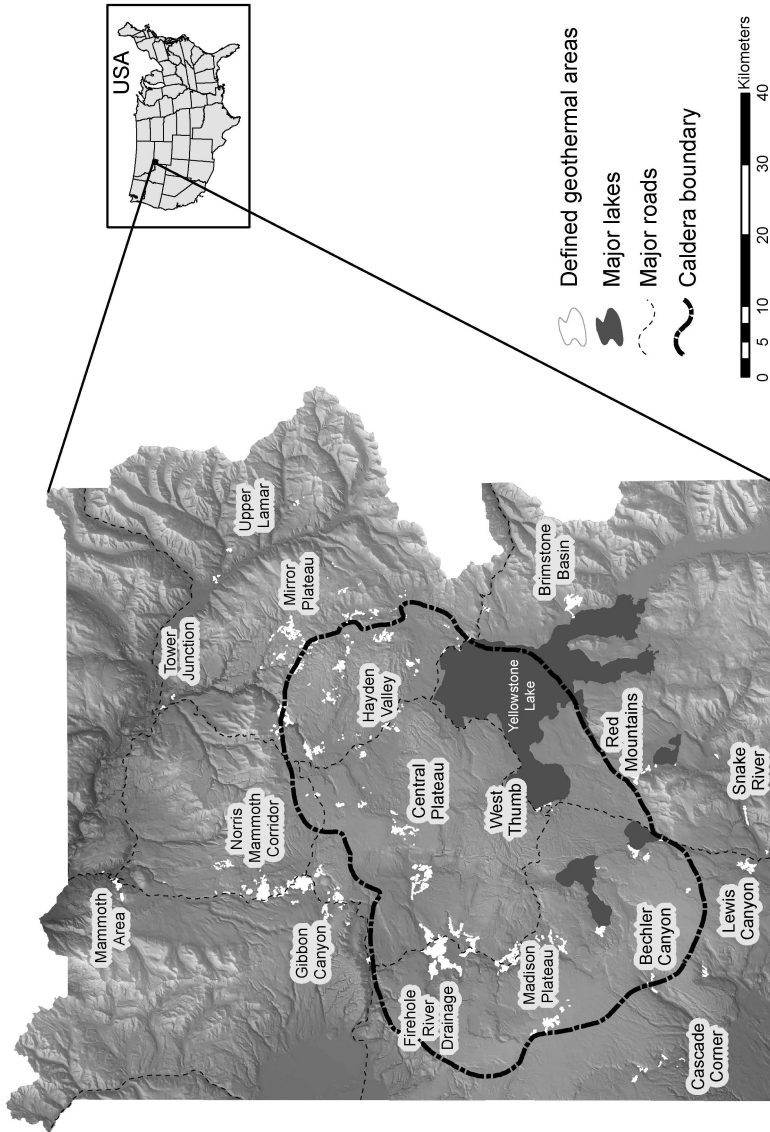


Fig. 1. Location map for Yellowstone National Park and the currently defined geothermal areas displayed with a shaded relief background. Spatial groupings discussed in the article are indicated with highlighted text.

Table 1. Landsat Images Used in the Study

Acquisition date (1980s)	Sensor	Acquisition date (1990s)	Sensor	Acquisition date (2000s)	Sensor
July 17, 1986	TM5	15 July 1991	TM5	July 15, 2000	ETM+
August 2, 1989	TM4	12 July 1996	TM5	July 2, 2001	ETM+
		15 July 1997	TM5	July 5, 2002	ETM+
		18 July 1998	TM5	August 1, 2003	TM5
		13 July 1999 ^a	ETM+	July 21, 2005 ^a	TM5
				July 8, 2006	TM5
				June 25, 2007	TM5

^aIndicates cloud-free image.

were acquired (Table 1). These images were chosen based on snow-free summer anniversary dates and lack of clouds. Image dates range from June 25 to August 2, resulting in anniversary dates within 5-½ weeks of one another. Two of the images are cloud free, while the remaining 12 have less than 5% cloud cover. Imagery was not acquired for several years during the study period due to lack of acceptable image quality.

Several ancillary data sets were required for analysis. Digital spatial data of the defined geothermal areas were provided by YNP. Digital spatial hydrology data were downloaded from the U.S. Geological Survey National Hydrology Dataset (NHD) (USGS, 2008). Geologic fault data were downloaded from a USGS Open File Report (Christiansen and Wahl, 1999). Earthquake data were downloaded for all years in the study from the Yellowstone Volcano Observatory/University of Utah Earthquake Information Center (University of Utah, 2009). Information included with each earthquake was location, date, time, and magnitude. Magnitude values were converted to linear amplitude by taking 10 to the power of the magnitude (i.e., if the magnitude was 2.24, amplitude = $10^{2.24} = 173.78$). Average air temperature and precipitation information was downloaded from the Canyon SNOTEL (SNOWpack TELEmetry) site, because it was the station nearest the center of YNP that had data for the entire study period (NRCS, 2009).

Image Preprocessing

Geometric registration of all images is vital when comparing different images in a change analysis. A “master” TM image (7 September 2005) was chosen that aligned well with National Agriculture Imagery Program (NAIP) imagery (root mean square error [RMSE] = 0.4128 pixels, or less than 15 m) and roads and trails data recorded with high-precision GPS units by YNP staff. The 14 summer images used for this project were geometrically registered to the master image based on the 30×30 m reflective bands, with an RMSE for each registration of less than 0.5 pixels (15 m).

Each image was clipped to the defined geothermal area boundaries study area. Clouds and snow were masked manually through on-screen digitizing. M_{terr} was calculated from the red, near-infrared (NIR), and thermal-infrared (TIR) Landsat bands using the methods described in Savage et al. (2010), including atmospheric and

radiometric correction (Chavez, 1996; Utah State University, 2008) and integration over the bandwidth (from 10.4 μm to 12.5 μm = 2.1 μm) and the projected solid angle of the hemisphere (π sr) (Savage et al., 2010). All resulting M_{terr} images had 120 m spatial resolution.

Thirteen M_{terr} difference (ΔM_{terr}) images were created by computing the absolute value of the difference in pixel values from one date to the next. Absolute difference was calculated rather than relative difference because change in any direction would be informative to the main questions of the study, and it is possible that triggers of geothermal change might cause increases in heat flow in some areas and decreases in others.

The sensitivity of calculated M_{terr} to a change of one raw digital number (DN) (the original Landsat band values that range from 0 to 255) was calculated by finding the average value of M_{terr} change per one DN change for each year. This sensitivity value is highly dependent on actual ground temperature, inasmuch as emittance is related to temperature to the 4th power in the Stefan-Boltzman Law ($M = \epsilon\sigma T^4$, where M is emittance, ϵ is emissivity, σ is the Stefan-Boltzman constant $5.67 \times 10^{-8} \text{ Wm}^{-2}\text{K}^{-4}$, and T is temperature in Kelvin); thus sensitivity was calculated by finding the difference in M_{terr} for all pairs of DNs with a difference of one, then averaging those differences across the image.

Change Analysis

Any pixel covered with snow or clouds in any of the 14 images was excluded from the change analysis. Twenty spatial groupings, each defined by YNP as "gross location of the thermal area within the park" (Spatial Analysis Center, 2005) and encompassing no less than 144,000 m^2 , were analyzed. Summary statistics of the groupings were tabulated and graphed to examine the data for trends over the 21-year period. The spatial grouping means were adjusted by subtracting the mean M_{terr} value for each date in order to account for overall trends in the data and focus on geothermal change. Linear regression models were computed with the mean M_{terr} as the response variable and air temperature and precipitation from Canyon SNOTEL data as the predictor variables to determine correlation. The trajectories of individual groupings were examined visually for trends or anomalous patterns. Several of the groupings were selected for additional analysis to compare to one another over the 21-year period because of their hypothetical relationships or lack thereof. For example (Fig. 1), it is speculated that Mammoth Hot Springs (in the Mammoth Area spatial group) and Norris Geyser Basin (in the Gibbon Canyon spatial group) "share plumbing" (Bargar, 1978; White et al., 1988). It is also speculated that geothermal activity within the caldera differs from that without (Pierce and Morgan, 1992; Morgan et al., 2003).

Comparison to Known Change Events

Where change has been documented (Table 2), 9 pixels (1 pixel where the feature resides and the 8 surrounding pixels) were extracted from each date in the 14-component multitemporal image to examine their trajectories against known change. These data were adjusted in the same manner as the spatial groupings. Graphs of the adjusted M_{terr} over time were plotted and examined for expected trajectories of change. These were

Table 2. Known Change Events in Geothermal Activity in Yellowstone National Park

Date(s) of change	Location of change	Description of change
Summer 1998	Narrow Gauge Spring in Mammoth Area Group	New feature appeared and began spreading over trail
1999	Minerva Terrace in Mammoth Area Group	Water stopped flowing and heat was no longer emitted
July 2003	Porkchop Geyser in Gibbon Canyon Group	Increased ground temperature; trail closed and rerouted
July and September 2006	Jewel Geyser in Firehole River Drainage Group	Possible hydrothermal explosions

also compared to the trajectory of the average of 9 random pixels from Brimstone Basin, where there has been no geothermal heat emitted for over 100 years (Langford, 1972), and therefore very little change should be observed. In addition, GHF was calculated for Brimstone Basin, using the methods published in Savage et al. (2010) and adjusted in the same manner as above so its trajectory could be compared to the adjusted M_{terr} trajectory to verify that M_{terr} was the appropriate choice of model to use for change analysis.

All of the geothermal features used in this analysis are considerably less than one pixel in extent. There are several potential barriers to the study of known change events with Landsat data. The changes witnessed on the ground in features that are only meters in size might not be discernable in a 120×120 m pixel. The changes also might not be detectable with the temporal resolution used. The changes might have lasted only days, weeks, or months, but not have occurred near enough to an image date to be sensed by the Landsat sensor. These features, although much smaller than the spatial resolution of Landsat data, were inspected to determine whether Landsat data were sensitive enough to detect these known changes and possibly other undocumented changes.

Spatial Pattern Analysis

Several images were created that represented distance to potentially important features, including geologic faults, large water bodies (defined as at least $14,400 \text{ m}^2$ or one 120×120 m pixel), and earthquake swarms. The linear nature of geologic faults, if associated with M_{terr} , might be visible in the spatial patterns of M_{terr} . During periods of drought, large water bodies might be the best source of groundwater recharge; thus, increased distance from large water bodies could affect the spatial patterns of M_{terr} . Earthquakes, both near and far, have been shown to affect the behavior of geothermal features in YNP (Rojstaczer et al., 2003; Husen et al., 2004).

Earthquake swarms are typically defined as a group of consecutive seismic events within a relatively short time period with no identifiable main shock (Spicak, 2000). For this study, in order to find at least one swarm per year, earthquake swarms were defined as (a) three or more earthquakes of any magnitude (b) within one week of each other (c) in an obvious visual spatial cluster (d) with a maximum distance between earthquakes of 3 km and (e) a lag time between the last earthquake and the image date

of no more than 100 days (in order to observe expected ground water changes for several weeks to months after an earthquake [Rojstaczer and Wolf, 1992; Rojstaczer et al., 1995]). The output values of the distance images represented the distance in number of pixels to the nearest feature (e.g., earthquake swarm) of interest. Mean distances to the features were tabulated for the 20 spatial groupings to determine which spatial groupings were nearest to the potentially important features of interest.

Three or more earthquake swarms were identified for each of 12 study years, totaling 71 swarms (Table 3). We did not analyze any swarms from 1986, because it was the earliest M_{terr} image and there was no earlier image from which to assess change, or for 1989 because there were no earthquakes that fit the definition of a swarm during that year. An image was created in which each pixel represented the distance from the boundary of each swarm for each of the 71 swarms and subsequently clipped to the spatial groupings boundaries so that the number of pixels to be examined was 7431.

The correlation of earthquake swarm characteristics to ΔM_{terr} was tested with regression analyses of spatial grouping swarm data that had seven predictor variables (distance to swarm, number of earthquakes in the swarm, maximum amplitude, mean amplitude, median amplitude, duration of the swarm, and lag time between final earthquake and image date) and one response variable (ΔM_{terr}), with data from all spatial groupings included in each model. All 71 swarms could not be used in one regression analysis because multiple swarms per year would not add true variance, but instead duplicate the response variable. The most important swarm per year, therefore, was chosen for eight different backwards and forwards stepwise regression analyses based on the following selection criteria: (1) most earthquakes, (2) highest maximum amplitude, (3) highest mean amplitude, (4) highest median amplitude, (5) longest duration of swarm, (6) shortest duration of swarm, (7) longest lag time, and (8) shortest lag time.

RESULTS

Terrestrial Emittance

The highest M_{terr} value calculated for all the study years was the maximum for 1999 at 440.53 Wm^{-2} , while the lowest value was the minimum for 1986 at 306.21 Wm^{-2} (Table 4). The temporal patterns seen in the Firehole River Drainage Group provide a visual example of the patterns that were consistent for all groups (Fig. 2). The highest average M_{terr} value was 389.62 Wm^{-2} in 2000. The general pattern of mean M_{terr} values shows an increase up to 2000 and a subsequent decrease.

Change Analysis

The average sensitivity of M_{terr} for a change of one DN over the 14 years of imagery was 1.14 Wm^{-2} . The sensitivity ranged from -18.35 to 16.38 Wm^{-2} . The negative sensitivity values likely were a result of unaccounted-for emissivity differences at each pixel. The overall trend of the spatial groupings showed increases of approximately 20 to 40 Wm^{-2} from 1986 to 2007 (Fig. 3). Part of the overall trend might be explained by differences in air temperature. The average temperature in $^{\circ}\text{C}$ for the week prior to the date of each image was obtained from the Canyon SNOTEL

Table 3. Earthquake Swarm Information by Year^a

Year	Number of swarms	Highest number of earthquakes	Highest maximum amplitude	Highest mean amplitude	Highest median amplitude	Longest duration (days)	Shortest duration (days)	Longest lag time (days)	Shortest lag time (days)
2007	5	26	43.65	17.92	12.17	28	1	79	5
2006	8	76	316.23	23.79	7.85	23	1	94	5
2005	6	49	812.83	79.85	31.62	16	1	91	5
2003	6	14	28.84	14.84	14.13	22	1	81	8
2002	8	31	34.67	18.95	20.42	16	1	98	4
2001	8	39	302.00	243.11	234.42	24	1	73	2
2000	5	30	9,549.93	1,121.52	138.04	20	1	51	3
1999	7	746	17,782.79	1,670.22	251.19	30	1	82	1
1998	3	39	758.58	284.32	269.15	15	1	38	2
1997	7	356	48,977.88	1,087.12	691.83	37	1	68	1
1996	5	25	6,918.31	1,928.03	758.58	21	1	47	1
1991	3	7	1,023.29	462.05	338.84	2	1	72	5

^aValues were derived from information from each of the 71 earthquake swarms.

Table 4. Summary Statistics of Terrestrial Emittance (M_{terr}) Calculations in the Defined Geothermal Areas for Each of the 14 years in the 21-Year Study Period (Wm^{-2})^a

Year	Min	Max	Mean	Median	Mode	Std. Dev.
1986	306.21	384.84	328.17	328.32	324.64	7.68
1989	310.34	402.57	338.10	336.64	338.44	12.37
1991	324.80	414.57	361.96	360.57	351.45	13.19
1996	322.72	399.77	359.09	358.24	368.77	13.41
1997	313.82	412.18	355.84	354.55	363.38	11.98
1998	325.28	424.73	369.23	368.01	378.11	12.43
1999	336.70	440.53	386.95	386.18	386.59	14.81
2000	343.55	436.98	389.62	388.81	381.87	14.32
2001	314.83	440.28	382.79	381.48	374.62	14.84
2002	331.11	426.66	377.11	376.27	375.90	14.73
2003	331.01	434.25	372.87	372.14	379.00	14.34
2005	321.32	427.22	378.01	376.75	373.86	14.82
2006	325.74	409.08	359.08	358.94	364.48	11.09
2007	313.55	413.58	359.76	359.66	359.66	10.81

^aA pattern emerges, with a general increase in M_{terr} up to 2000 followed by a general decrease in M_{terr} .

data (Table 5). A linear regression model with mean M_{terr} as the response variable and the SNOTEL air temperature as the predictor variable was computed for the spatial groupings. The resulting R^2 for spatial groupings was 0.26. When percent of normal year-to-date precipitation for the image date was added to either regression, there was little improvement.

The M_{terr} data were adjusted by removing the background variability explained by air temperature as well as other unknown factors by subtracting M_{terr} date means from the group means (Fig. 4). The spatial groupings showed more variability after adjusting for background effects. The Tower Junction spatial group appeared to have the largest variation of the spatial groupings (lowest measurement of -4 Wm^{-2} in 1996 and highest measurement of 21 Wm^{-2} in 1989), with a range of 24.8 Wm^{-2} (Fig. 4).

Adjusted trajectories for spatial groupings were compared by suggested relationships for further examination of trajectories. The spatial grouping trajectories appeared to show dramatic differences between spatial groupings (Fig. 4), although, after further visual inspection of the images, most of these changes did not represent dramatic visual differences on the ground (e.g., dead vegetation where M_{terr} increased substantially).

The Gibbon Canyon group and the Norris Mammoth Corridor group appear to have similar trajectories over the 21-year period, with slight differences in direction from 1991 to 1996 and 2003 to 2005, and a correlation of 0.80 (Fig. 5A). The Mammoth Area group trajectory, on the other hand, is not similar to, and has low correlations with, the Gibbon Canyon (-0.14) and Norris Mammoth Corridor (0.15)

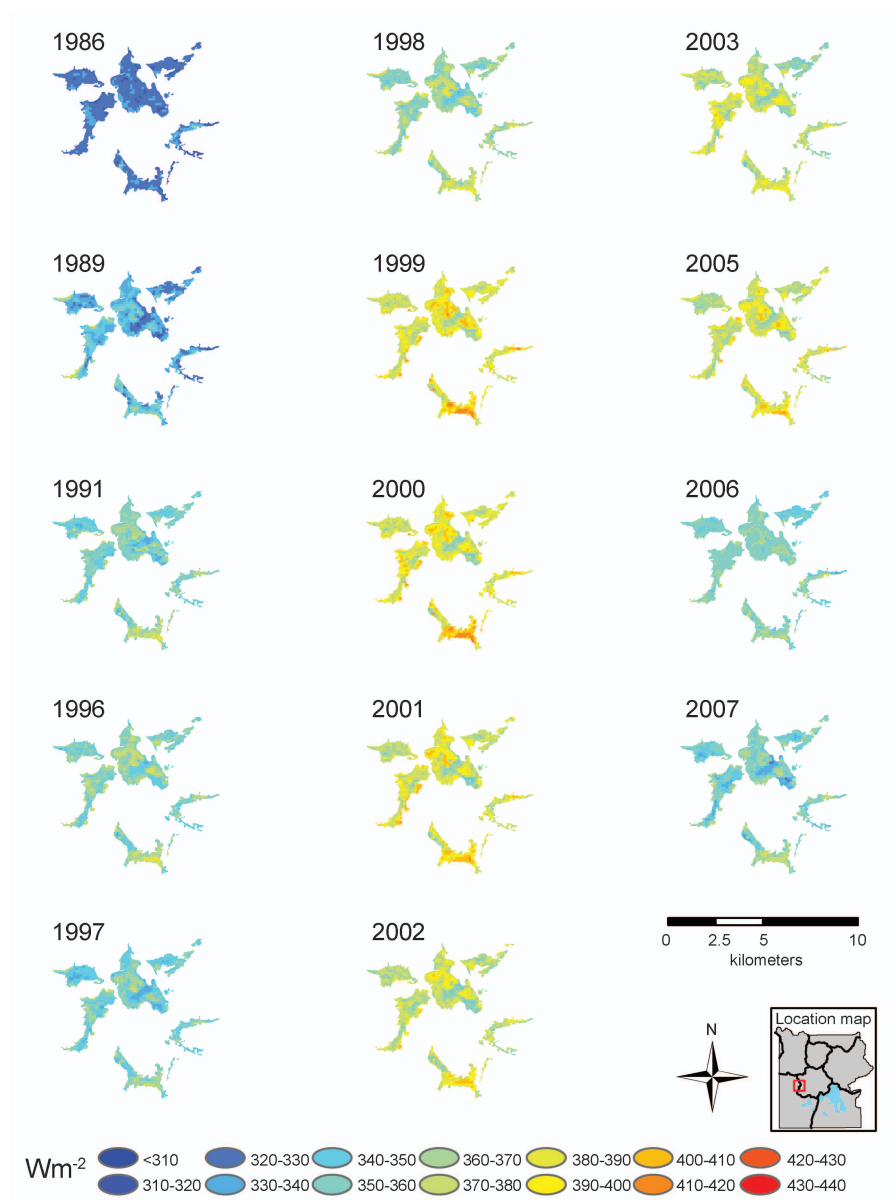


Fig. 2. Terrestrial emittance (M_{terr}) values for Lower Geyser Basin (in the Firehole River Drainage Group) for each of the 14 years in the 21-year study period. The same pattern seen in all spatial groupings emerges with a general increase in M_{terr} up to 2000, followed by a general decrease in M_{terr} .

trajectories. The trajectories of the Firehole River Drainage group that lies completely within the caldera boundary and the Gibbon Canyon group that lies completely outside the caldera boundary (Fig. 1) have a correlation of -0.24 , yet are similar in that both are warmer than average (except for the first two negative values for Gibbon Canyon; Fig. 5B). The trajectories are also similar in direction of change from 1997 to 2000, but

Table 5. Average Terrestrial Emittance (M_{terr}) in Wm^{-2} , Air Temperature in $^{\circ}\text{C}$, and Percent of Normal Precipitation for 14 Image Dates

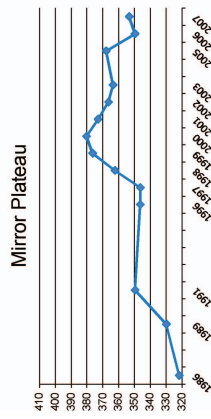
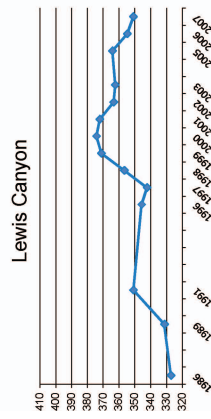
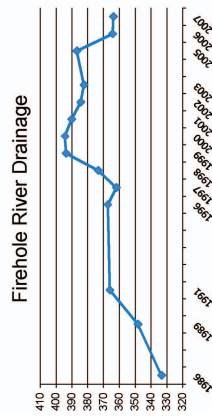
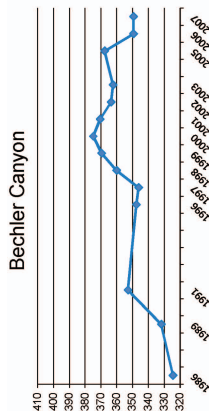
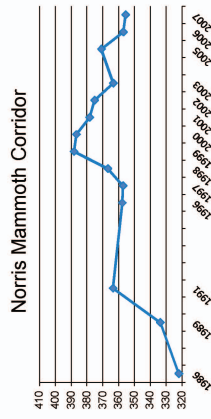
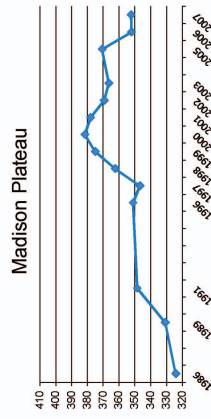
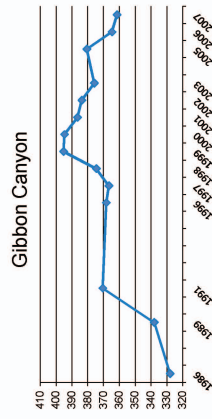
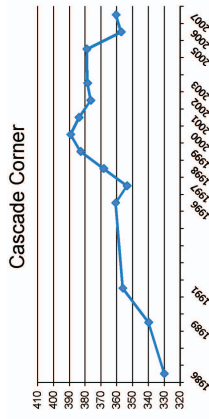
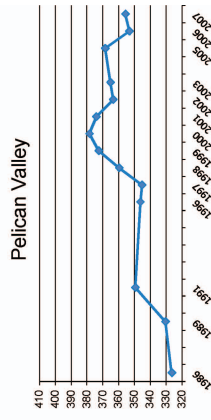
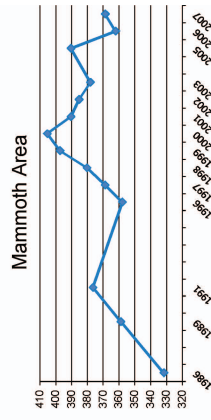
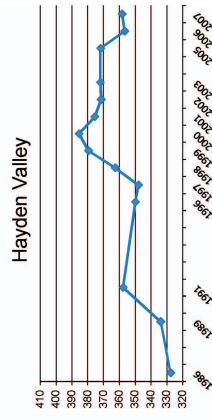
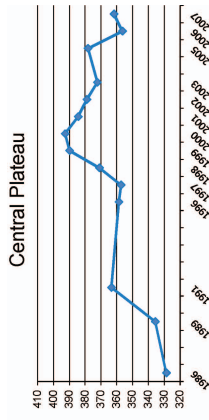
Date	M_{terr} spatial groupings	Temperature	Pct. precipitation
August 2, 1989	338.2	12.9	100.0
July 15, 1991	362.0	12.0	103.1
July 12, 1996	359.2	13.8	130.4
July 15, 1997	356.0	10.5	139.3
July 18, 1998	369.3	14.9	97.2
July 13, 1999	387.2	13.3	112.7
July 15, 2000	389.8	13.8	96.5
July 2, 2001	382.9	15.0	81.8
July 5, 2002	377.3	14.9	94.4
August 1, 2003	372.9	16.0	84.5
July 21, 2005	378.0	15.5	76.6
July 8, 2006	359.0	13.4	91.9
June 25, 2007	359.8	12.6	85.7

have few similarities beyond this. The trajectories of the Lewis Canyon group (outside the caldera) and the Madison Plateau group inside the caldera (Fig. 1) have a correlation of 0.53 and are similar in that they are both negative values and have almost identical directions of change (Fig. 5C). The differences lie in the direction of change between 1991 and 1996 and the magnitude of change, especially from 2005 to 2006.

Comparison to Known Change Events

Institutional knowledge of changes in geothermal activity was compared to changes in M_{terr} values over time. A large spring near Narrow Gauge in the Mammoth Area group (Fig. 1) appeared during the summer of 1998. An increase in M_{terr} from 1998 to 1999 was observed at Narrow Gauge and surrounding areas (Fig. 6A). Water stopped flowing and steam stopped being emitted at Minerva Terrace in 1999, also in the Mammoth Area group. It remains inactive at present (February 2012). A decrease in M_{terr} from 1998 to 1999 was observed at Minerva Terrace, with a very slight decrease in the surrounding area (Fig. 6B).

The ground near Porkchop Geyser in the Gibbon Canyon spatial group (Fig. 1) increased in temperature enough that YNP staff were required to close parts of the path and build boardwalks so visitors would not burn their feet during the summer of 2003. A decrease in M_{terr} from 2002 to 2003 and a very slight decrease from 2003 to 2005 were observed in the pixel that contained Porkchop Geyser, while there was a slight increase from 2003 to 2005 in the surrounding area (Fig. 6C). It is unknown whether an increase occurred between 2003 and 2004 because of the lack of imagery from 2004. Both the pixel that contained Porkchop Geyser and the surrounding area showed a large increase from 2005 to 2006.



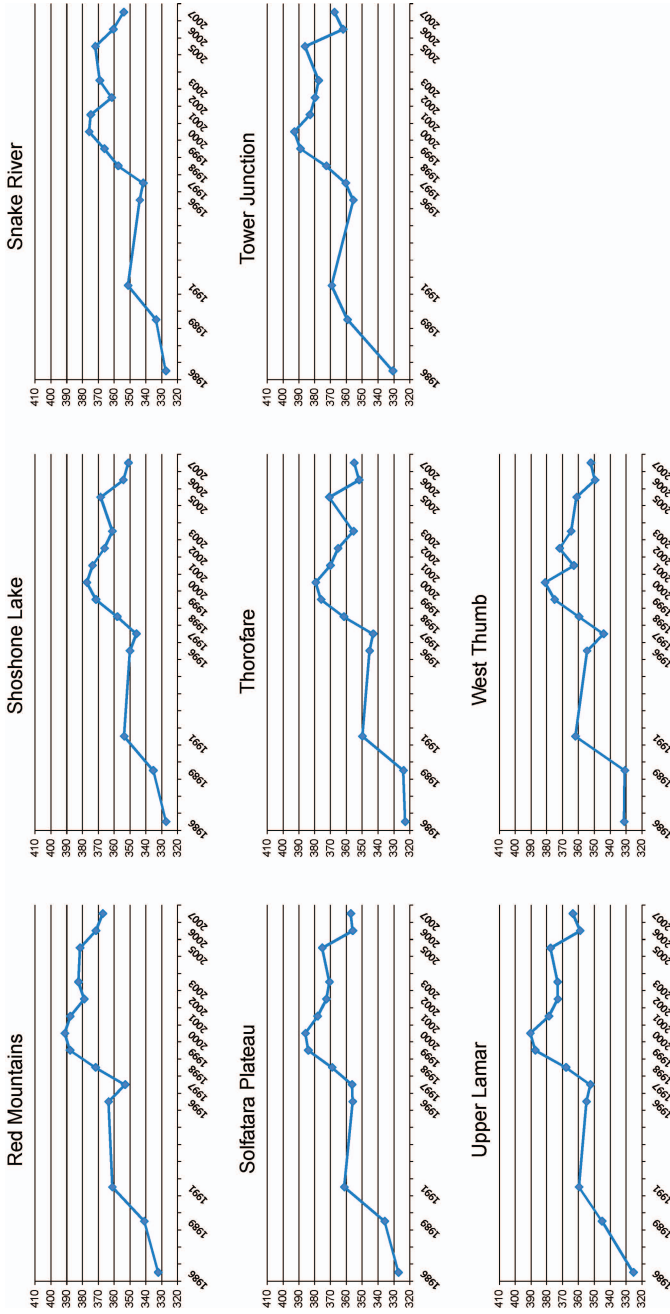
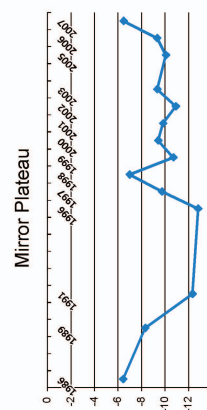
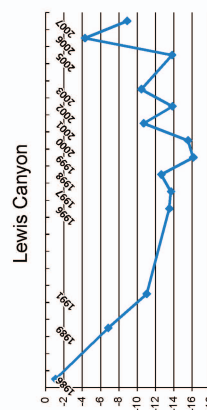
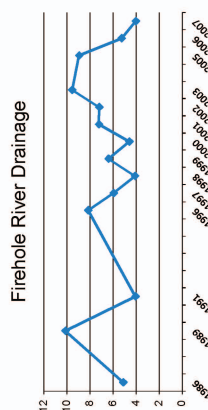
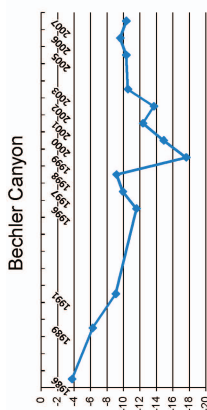
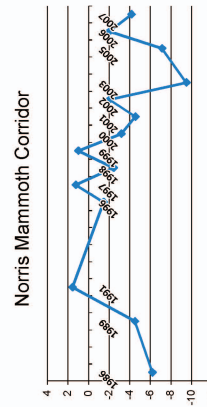
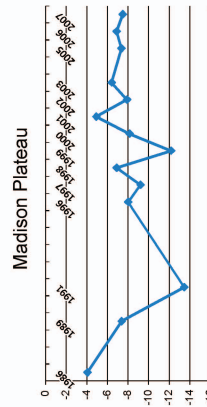
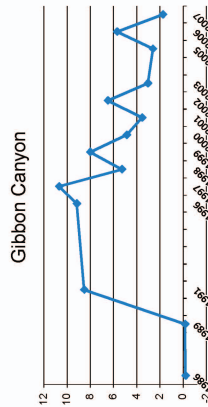
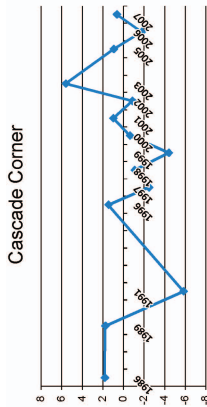
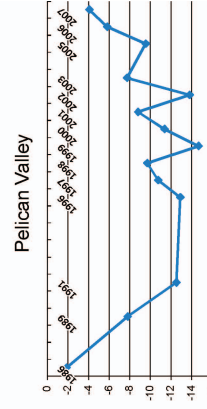
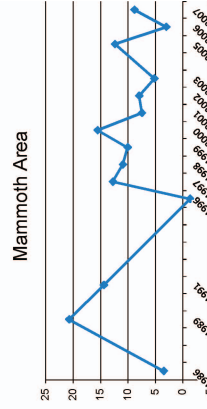
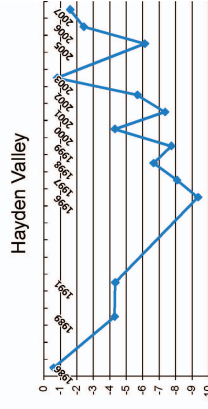
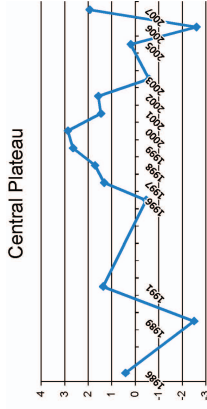


Fig. 3. Trajectories of 20 spatial groupings of 14 dates of terrestrial emittance (M_{ter})(Wm^{-2}). Each trajectory follows a similar general pattern, increasing to 2000 and decreasing to 2007.



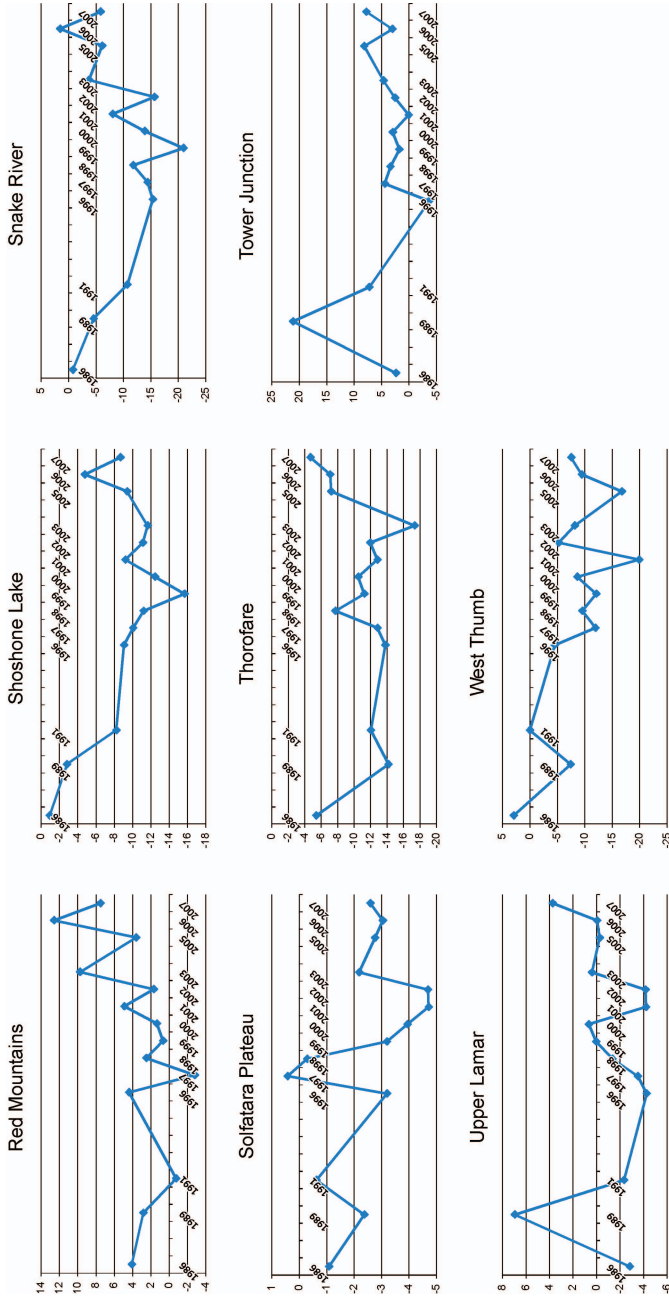


Fig. 4. Trajectories of 20 spatial groupings, adjusted by terrestrial emittance (M_{ter}) date mean. Y-axis is difference from the date mean in Wm^{-2} . The Tower Junction group appears to have the largest variation with a range of $24.8 Wm^{-2}$.

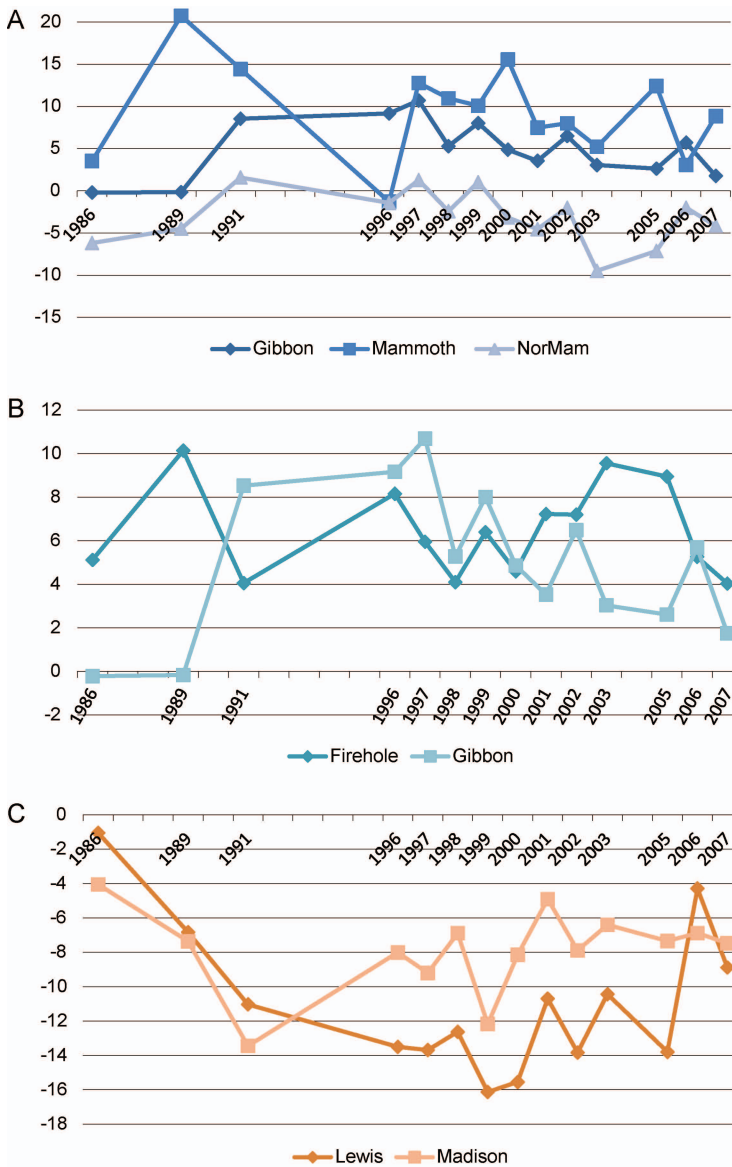


Fig. 5. Adjusted terrestrial emittance (M_{terr}) trajectories for (A) Gibbon Canyon, Mammoth Area, and Norris-Mammoth Corridor; (B) Firehole River Drainage and Gibbon Canyon; and (C) Lewis Canyon and Madison Plateau. Y-axis is difference from the date mean in Wm^{-2} .

Possible hydrothermal explosions occurred near Jewel Geyser in the Firehole River Drainage spatial group (Fig. 1) on July 14, 2006 and September 23, 2006. The 2006 Landsat image was acquired on July 8, six days prior to the first geothermal event. A decrease in M_{terr} values near Jewel Geyser from 2005 to 2006 and a continued but less significant decrease from 2006 to 2007 were observed, while the pixel that contained Jewel Geyser increased slightly from 2006 to 2007 (Fig. 6D).

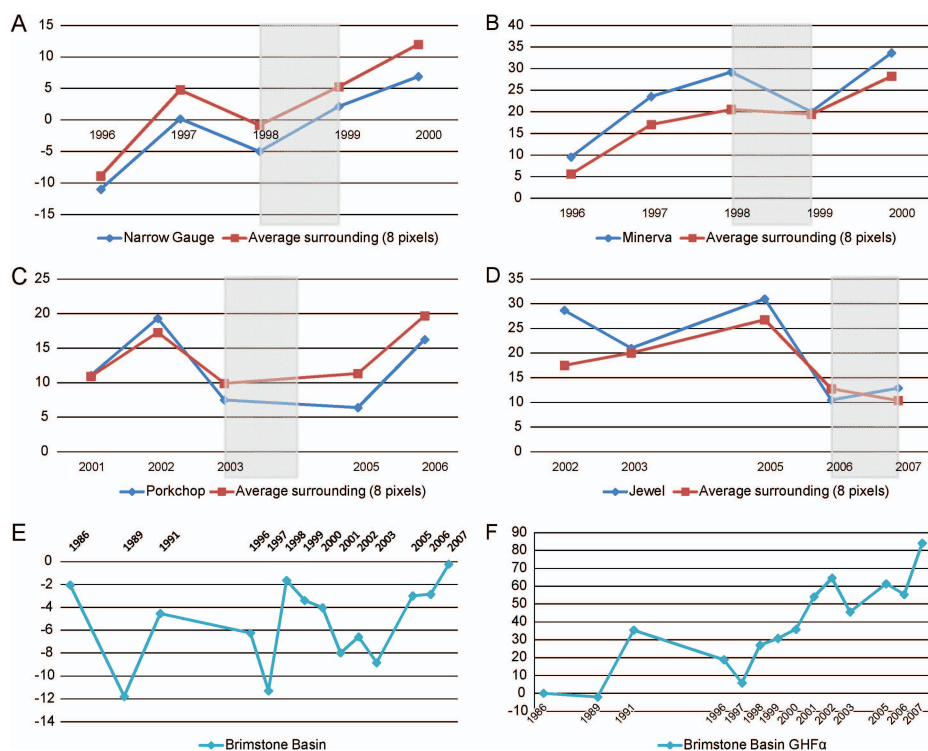


Fig. 6. Changes in terrestrial emittance (M_{terr}) at (A) Narrow Gauge in the Mammoth Area Group, (B) Minerva Terraces in the Mammoth Area Group, (C) Porkchop Geyser in the Gibbon Canyon Group, (D) Jewel Geyser in the Firehole River Drainage Group, (E) Brimstone Basin, and (F) Brimstone Basin GHF. Y-axis is difference from the date mean in Wm^{-2} . Known change events are highlighted in grey.

Brimstone Basin (Fig. 1) was geothermally inactive during the study period, and therefore should have relatively constant emittance, except for solar radiation effects, but does indicate some M_{terr} variability during the study period (Fig. 6E). Brimstone Basin had the smallest range of values as well as the smallest mean when the ranges of change and means of M_{terr} for the five locations above were compared (Table 6). The range of change of GHF in Brimstone Basin, however, was nearly eight times larger than that of M_{terr} (Table 6) and the trajectory had a distinct upward trend (Fig. 6F).

Spatial Pattern Analysis

Each of the 20 spatial groupings were mostly contiguous (i.e., one polygon each), but several groups were highly dispersed across the landscape (e.g., Central Plateau and Mirror Plateau) (Fig. 1). The Red Mountains spatial grouping was on average the closest to geologic faults at 309 m, with the Cascade Corner group on average the farthest away at 11,845 m, with the average distance of all spatial groupings to geologic faults being 3180 m. The Red Mountains group had a slightly linear shape and was intersected by faults. The Cascade Corner group also had a slightly linear shape; however, there were no faults in the vicinity of this group.

Table 6. Summary Statistics of Changes in Terrestrial Emittance (M_{terr}) for 1 Pixel and 9 Pixels Surrounding Narrow Gauge (NG), Minerva Terrace (Min), Porkchop Geysir (PC), and Jewel Geysir (Jwl)^a

	NG (1)	NG (9)	Min (1)	Min (9)	PC (1)	PC (9)	Jwl (1)	Jwl (9)	Brs M_{terr}	Brs GHF
Min	-10.99	-9.10	2.44	2.78	1.05	5.57	10.50	7.49	-11.80	-2.03
Max	12.86	13.84	33.66	28.79	24.47	21.15	30.97	29.91	-0.22	84.05
Mean	-1.29	2.09	20.71	17.16	11.28	13.38	20.75	18.91	-5.32	36.94
Range	23.85	22.93	31.22	26.01	23.43	15.58	20.47	22.42	11.58	86.08

^aAlso presented are terrestrial emittance (M_{terr}) and albedo and potential annual direct incident solar radiation corrected geothermal heat flux (GHF) of 9 pixels in Brimstone Basin (Brs). Values are the difference from the date mean in Wm^{-2} .

The Snake River spatial grouping was on average the closest to large water bodies at 78 m, with the Bechler Canyon group on average the farthest away at 5458 m, and the average distance of all spatial groupings to large water bodies was 1563 m. The Snake River group follows the Snake River for the most part. The Bechler Canyon group is in the southwest corner of YNP and very distant from most large water bodies (Fig. 1).

The Hayden Valley spatial grouping was on average the closest to earthquake swarms at 1412 m, with the Upper Lamar group on average the farthest away at 30,233 m, and the average distance of all spatial groupings to earthquake swarms was 9547 m. The Hayden Valley group is intersected by swarms from 2002 and 2005. The Upper Lamar group is in the northeast portion of YNP and very distant from any of the earthquake swarms.

Eight swarm characteristics were used to choose one swarm per year for multitemporal linear regression analyses. The resulting R^2 values for the eight analyses ranged from 0.15 to 0.34 (Table 7). The best model, with an R^2 of 0.34, was based on the longest lag time between the last earthquake in a swarm and the image date.

DISCUSSION AND CONCLUSION

Geothermal areas of YNP can range from highly stable to extremely dynamic. Landsat data were evaluated for their ability to detect change over a 21-year period in the defined geothermal areas of YNP. Trajectories of mean M_{terr} values were plotted across time and evaluated for spatial and temporal patterns of change. Locations where change had been observed were inspected in more detail. Spatial patterns of absolute change in M_{terr} were evaluated for correlations with distance to several natural features: geologic faults, large water bodies, and earthquake swarms.

Terrestrial Emittance

Reasonable estimates of terrestrial emittance that did not account for effects from solar radiation were produced from all 14 images (Table 4), and change in M_{terr} was examined over these 14 dates. The same processes were completed for every image

Table 7. R^2 values of Different Combinations of “Best” Swarm per Year^a

Criteria for “best” swarm	R^2
Longest lag time	0.34
Quakes per swarm	0.26
Maximum amplitude	0.26
Longest duration	0.25
Mean amplitude	0.21
Shortest duration	0.18
Median amplitude	0.16
Shortest lag time	0.15

^aThe longest lag time had the highest R^2 value, explaining over one-third of the variation.

in this project. Even with solar radiation not taken into account, the M_{terr} values across time were comparable with this method because a change analysis on these data would indicate relative change rather than absolute change. In other words, the relative solar effects were expected to be similar across time because they are primarily a function of constants (e.g., slope, aspect, and elevation), so observed differences should be due to geothermal change.

Image-to-image registration errors, however, might induce some errors in change analysis. For example, a feature with high M_{terr} might be at the edge of a pixel and thus change location due to registration error between two dates, resulting in a large, possibly false change at that pixel. Registration error might limit the utility of change analysis at the pixel level, but broader patterns of change are still apparent.

The general trend of all M_{terr} data was the same: increasing until the year 2000, with a subsequent decrease (Fig. 3). This trend was demonstrated in every part of the defined geothermal areas. The trend is consistent with a hypothesized cyclical pattern in terrestrial emittance in YNP, as is found in resurgent domes within the 640,000-year-old caldera (Brantley et al., 2004), although the study period might not have been long enough to observe a full cycle of terrestrial emittance change. Thirty years of caldera measurements indicated a pattern of uplift from 1973 to 1985, subsidence to 1996, then uplift again to 2003 (Brantley et al., 2004; Chang et al., 2007). This pattern is not the same as the patterns observed in this study, but it does indicate cyclical tendencies in geothermal activity.

As previously noted, it has been suggested that Norris Geyser Basin and Mammoth Hot Springs share “plumbing” to some degree (Bargar, 1978; White et al., 1988). A comparison of M_{terr} trajectories of Mammoth Area, Norris Mammoth Corridor, and Gibbon Canyon (which includes Norris Geyser Basin) revealed that Gibbon Canyon and Norris Mammoth Corridor had almost identical trajectories, while the Mammoth Area trajectory had a very low correlation with the other two trajectories (Fig. 5A). Gibbon Canyon and Norris Mammoth Corridor are adjacent to one another and both are associated with a river (Gibbon Canyon with Gibbon River and Norris Mammoth

Corridor with Obsidian Creek). Mammoth Area, on the other hand, is over 13 km away from the bulk of Norris Mammoth Corridor and is not associated with a river.

Some have suggested that geothermal areas within the 640,000-year-old caldera boundary behave differently than geothermal areas outside of the boundary (Pierce and Morgan, 1992; Morgan et al., 2003). When the Firehole River Drainage and Madison Plateau trajectories (within the caldera boundary) were compared to the Gibbon Canyon and Lewis Canyon trajectories outside of the caldera boundary (Fig. 1), few similarities in temporal patterns were observed (Figs. 5B and 5C). This could support the idea that there are differences in geothermal behavior on either side of the caldera boundary.

The change analysis should detect change in geothermal areas of various sizes, so it was important to determine what the sensitivity to change was for Landsat thermal pixels. When the raw DN changes by 1, the M_{terr} values change on average by 1.14 Wm^{-2} . This means, for example, that a feature the size of Excelsior Geyser in Lower Geyser Basin in the central portion of the Firehole River Drainage spatial group (Fig. 1), one of the largest features in YNP at around 3000 m^2 , would have to change by 5.47 Wm^{-2} (or 0.68°C , assuming an initial temperature of 55.56°C , the recorded temperature from the YNP Thermal Inventory Project) to see a change of 1 raw DN in the 120 m pixel in which it resides. Excelsior Geyser would occupy only 21% of a 120 m Landsat thermal pixel. A larger feature, such as Grand Prismatic, the largest feature in YNP, at approximately $14,400 \text{ m}^2$ (adjacent to Excelsior Geyser), or a large area of geothermally active ground would need to change by 1.14 Wm^{-2} for the change to be detectable by Landsat. A small feature, such as Anemone Geyser near Old Faithful (in the southern portion of the Firehole River Drainage spatial group), which is approximately 1 m^2 , or a small area of geothermally active ground would need to change by over $16,000 \text{ Wm}^{-2}$ (assuming it is the only area within a pixel emitting heat). Temperature has a strong non-linear relationship to M_{terr} , and thus the Landsat thermal pixel sensitivity to change will differ for every feature or location not only because of size but also because of inherent temperature.

Known Change Events

Institutional knowledge, although inconsistent and not uniform in coverage, is one way to learn about geothermal activity in YNP. Institutional knowledge, combined with more consistent and uniform Landsat data, allows the study of documented changes over time. Geothermal features are constantly changing, sometimes in small ways, such as the periodicity of a geyser changing by one minute, and sometimes in spectacular ways, such as hydrothermal explosions. Some documented changes in geothermal areas during the study time period were observed in the change trajectories, while several were not detected with the Landsat data. The M_{terr} values of the feature near Narrow Gauge Geyser in the Mammoth Area group that appeared during the summer of 1998 showed a general increase from 1996 to 2000 with the biggest increase between 1996 and 1997 (Fig. 6A). The surrounding pixels had higher adjusted M_{terr} values, indicating that the entire area was in an upward trend. Minerva Terrace, also in the Mammoth Area group, stopped flowing and emitting heat and steam in 1999, and its M_{terr} decreased from 1998 to 1999, although it increased in 2000 (Fig. 6B). The trajectory for just the Minerva Terrace pixel is generally higher than the

surrounding pixels trajectory, except in 1999, when they are almost exactly the same. This might be a representation of its change from flowing to not flowing, although the M_{terr} values increased from 1999 to 2000 even though Minerva Terrace did not begin to flow again.

Porkchop Geysir in the Gibbon Canyon group showed a slight unexpected decrease in M_{terr} values from 2003 to 2005 (Fig. 6C), but it is unknown if M_{terr} actually increased or decreased in 2004. Thus no conclusion can be reached regarding whether the field-recorded increase in temperature in Norris Geysir Basin in 2003 can be sensed by Landsat data. The surrounding pixels had a slightly higher average adjusted M_{terr} than the pixel that contained Porkchop Geysir and also increased between 2003 and 2005, possibly indicating a larger area of increased heat and/or a pixel registration error. The increase in M_{terr} from 2005 to 2006 was not observed by YNP scientists on the ground and perhaps indicated the change seen in these trajectories was data noise rather than actual change in M_{terr} . The possible hydrothermal explosions near Jewel Geysir in the Firehole River Drainage group in 2006 appeared to be sensed in M_{terr} because the values increased slightly after 2006 for the pixel that contained Jewel Geysir, but not for the surrounding pixels (Fig. 6D). A recent (May 2009) hydrothermal explosion in the same area is consistent with the increase in M_{terr} after 2006.

Brimstone Basin, close to the shore of the southeast arm of Yellowstone Lake, appears to be an extinct geothermal area, yet it is included in the defined geothermal areas. The waters running out of the basin are acidic and sulfuric, however, the waters are not hot and there has been no steam witnessed in the area since before YNP was established in 1872 (Langford, 1972; Nordstrom et al., 2009). Very little change should have occurred in Brimstone Basin during the study period since it is a geothermally constant area emitting no heat. The M_{terr} trajectory graph for Brimstone Basin indicated year-to-year variability that might be more indicative of solar radiation issues rather than true increases and decreases in M_{terr} in the area (Fig. 6E). The degree of variability in M_{terr} at Brimstone Basin, however, was less than that of the features where true geothermal change was observed (Fig. 6 and Table 6), supporting the conclusion that little to no M_{terr} change should be observed there because it has been inactive for over 100 years.

The GHF values in Brimstone Basin were noticeably different from the M_{terr} values of the same pixels (Figs. 6E and 6F and Table 6). The GHF trajectory graph for Brimstone Basin showed large year-to-year variability and a wide range of values, in addition to an obvious upward trend (Fig. 6F). This suggests that the solar and albedo corrections used in the GHF model were inadequate and the use of M_{terr} for this change analysis was preferred.

Spatial Patterns

Negligible relationships were observed between some spatial groupings and geologic faults and large water bodies. The Red Mountains spatial grouping had a relationship with intersecting geologic faults, while the Snake River and Firehole River Drainage spatial groupings were adjacent to and intersected by large water bodies. There was no relationship with precipitation data, indicating that the effects of drought on M_{terr} are not detectable with Landsat data.

Recorded earthquakes have had almost immediate effects on geysers in YNP, specifically on their periodicity (Rojstaczer et al., 2003; Husen et al., 2004). This behavior might indicate that the fluid movement beneath the surface is affected by earthquakes, and thus the heat emitted from some geothermal features might change with ground movement associated with earthquakes. In order to investigate the multi-temporal spatial relationship of M_{terr} to earthquake swarms, one swarm was selected per year. The manner of choosing the swarms to include in the regression analyses is important. The eight regression models based on different swarm characteristics each explained over 10% of the between-date variation (Table 7), indicating that geothermal heat flux (as opposed to terrestrial emittance) is actually an important part of the change analyses, since earthquake swarms are unlikely to be correlated with solar inputs.

The regression model with the best predictive ability, based on longest lag time between last earthquake and image date, might be explained by the movement of fluid through the Earth's crust. Prior to an earthquake, the rock in the crust can be deformed and microscopic cracks spread. Water might fill in or escape through those cracks and water levels in wells might fluctuate (Roeloffs, 1988; Thompson and Turk, 2005). Earthquakes alter water levels in wells. As it takes time for geothermally heated groundwater to flow to surface features, earthquake-mediated ground water changes might not be observed at the surface until as much as a year after the earthquake (Rojstaczer et al., 1995). Thus, changes in hydrologic behavior from earthquakes might not be observable for some time after the earthquake. A relationship was observed between changes in M_{terr} and earthquake swarms that happened between 38 and 94 days prior to the image dates.

The lowest correlation found in this study between M_{terr} and earthquake swarms was on the combination of swarms that had the shortest lag time between the last earthquake and the date of the imagery (1 to 2 days prior to the image dates) (Table 7). If the hypothesis that the longest lag times have the strongest relationship because of hydrologic fluid movement is correct, a short lag time might not allow enough time for the fluid to move and create observable effects at the surface.

The remaining swarm characteristics explained additional variability in M_{terr} changes, with the number of earthquakes in each swarm showing the second best correlation at 0.27. This is not unexpected because the mean magnitude of all the earthquakes in the study was 1.58, defined as "micro" by the USGS and very rarely felt (USGS, 2009a, 2009b); therefore 746 earthquakes with "light" to "micro" magnitudes might have greater effects than 7 earthquakes with similar magnitudes. Magnitude (amplitude) and duration of swarm are, of course, important factors as well. When swarms were chosen based on maximum amplitude the correlation was 0.26, while the correlation was 0.25 when swarms were chosen for longest duration. These results also were not unexpected, because higher amplitude earthquakes might be expected to cause more disturbance than lower amplitude earthquakes, and when swarms last for several days there might be accumulated effects on the Earth's crust.

Implications

Calculated M_{terr} over time using Landsat imagery could be a useful tool for monitoring geothermal areas at YNP and elsewhere. The values are calculated in a consistent manner and are comparable over time. Using the 2007 M_{terr} values as a base

map, YNP scientists can continue looking at changes in terrestrial emittance over time with free Landsat data for the foreseeable future. The trajectory analysis of the spatial groupings provided insight into the spatial relationships (or lack thereof) of various defined geothermal areas within and outside of the 640,000-year-old caldera, as well as between Mammoth Hot Springs and Norris Geyser Basin. The effects of solar radiation might explain why Brimstone Basin registered as somewhat variable over time. Solar radiation remains a serious concern, as discussed in Savage et al. (2010), and should be accounted for, if possible, in future studies of this nature.

The results from this study indicate that spatial and temporal resolutions are important factors in calculating terrestrial emittance and analyzing change over time. This study focused on decadal change analysis and included data that could be used for research with smaller temporal ranges. Because Landsat ETM+ thermal data are available as 60×60 m pixels, it would be of interest to study ETM+ images only to see if change is better detected at a finer spatial resolution (four summer images are available from 1999 to 2002), although future Landsat thermal data from the Landsat Data Continuity Mission will have a spatial resolution of 100×100 m. The current dataset includes seven consecutive anniversary dates (within 16 days in July) from 1996 to 2002. Focusing a study on these dates might remove the effects of the non-consecutive dates and missing data.

Earthquake swarms, as defined in this project, have a clear relationship with absolute changes in M_{terr} , with earthquake swarms explaining over one-third of the variation in ΔM_{terr} . This relationship was studied without taking interactions between swarm characteristics into account (e.g., how maximum amplitude relates to number of earthquakes in a swarm). These interactions might prove important in the M_{terr} /swarms relationship and could be investigated further to improve the understanding of these complex geological relationships.

Changes in the defined geothermal areas of YNP often are not visible with the naked eye or with ground-based field methods. Earthquake swarms as defined for this study did have a significant correlation with the spatial patterns of change in geothermal areas. Further, more detailed studies of earthquake swarms and their effect on the behavior of geothermal areas and features might enable scientists at YNP to locate specific areas to study in more detail with on-the-ground field methods and/or higher spatial resolution airborne image analyses.

ACKNOWLEDGMENTS

The authors wish to extend their appreciation to Yellowstone National Park and its geologists, Hank Heasler and Cheryl Jawrowski, for their support of this project. Funding was provided by the National Park Service/Yellowstone National Park through Rocky Mountain CESU task agreement J1580050584. The views expressed in the paper do not necessarily represent the views of the agency or the United States Government.

REFERENCES

- Bargar, K. E., 1978, *Geology and Thermal History of Mammoth Hot Springs, Yellowstone National Park, Wyoming*, Washington, DC: U.S. Geological Survey Bulletin 1444, 55 pp.

- Barrick, K. A., 2010, "Environmental Review of geyser basins: Resources, Scarcity, Threats, and Benefits," *Environmental Review*, 18(1):209–238.
- Brantley, S. R., Lowenstern, J. B., Christiansen, R. L., Smith, R. B., Heasler, H., Waite, G., and C. Wicks, 2004, *Tracking Changes in Yellowstone's Restless Volcanic System*, Reston, VA: USGS Fact Sheet 100-03.
- Brunsell, N. A. and R. R. Gillies, 2002, "Incorporating Surface Emissivity into a Thermal Atmospheric Correction," *Photogrammetric Engineering & Remote Sensing*, 68(12):1263–1269.
- Bryan, T. S., 2008, *The Geysers of Yellowstone* (4th Ed.), Boulder, CO: University of Colorado Press, 462 pp.
- Chang, W., Smith, R. B., Wicks, C., Farrell, J. M., and C. M. Puskas, 2007, "Accelerated Uplift and Magmatic Intrusion of the Yellowstone Caldera, 2004 to 2007," *Science*, 318(5852):952–956.
- Chavez, P. S. J., 1996, "Image-Based Atmospheric Corrections—Revisited and Revised." *Photogrammetric Engineering & Remote Sensing*, 62(9):1025–1036.
- Christiansen, R. L. and R. R. Wahl, 1999, *Digital Geologic Map of Yellowstone National Park, Idaho, Montana, Wyoming and Vicinity*, Reston, VA: U.S. Geological Survey, Open-File Report 99-174.
- Custer, S. G., Michels, D. E., Sill, W., Sonderegger, J. L., Weight, W., and W. Woessner, 1993, *Recommended Boundary for Controlled Groundwater Area in Montana Near Yellowstone Park*, Fort Collins, CO: U.S. Department of the Interior National Park Service, 29 pp. [<http://www.archive.org/stream/recommendedbound00custrich#page/n0/mode/1up>], last accessed May 19, 2011.
- Dobson, P. F., Kneafsey, T. J., Hulen, J., and A. Simmons, 2003, "Porosity, Permeability, and Fluid Flow in the Yellowstone Geothermal System, Wyoming," *Journal of Volcanology and Geothermal Research*, 123(3–4):313–324.
- Finn, C. A. and L. A. Morgan, 2002, "High-Resolution Aeromagnetic Mapping of Volcanic Terrain, Yellowstone National Park," *Journal of Volcanology and Geothermal Research*, 115(1–2):207–231.
- Fournier, R. O., 1989, "Geochemistry and Dynamics of the Yellowstone National Park Hydrothermal System," *Annual Reviews of Earth and Planetary Science*, 17:13–53.
- Fournier, R. O., Thompson, J. M., Cunningham, C. G., and R. A. Hutchinson, 1991, "Conditions Leading to a Recent Small Hydrothermal Explosion at Yellowstone National Park," *Geological Society of America Bulletin*, 103(8):1114–1120.
- Fournier, R. O., White, D. E., and A. H. Truesdell, 1975, "Convective Heat Flow in Yellowstone National Park," in *Proceedings of the Second United Nations Symposium on the Development and Use of Geothermal Resources*, 731–739.
- Friedman, I. and D. R. Norton, 2007, "Is Yellowstone Losing Its Steam?—Chloride Flux out of Yellowstone National Park," in *U.S. Geological Survey Professional Paper 1717*, 272–297.
- Hardy, C. C., 2005, *Characterizing Thermal Features from Multi-Spectral Remote Sensing Data Using Dynamic Calibration Procedures*, Missoula, MT: University of Montana, 153 pp.
- Harris, A. J. L., Flynn, L. P., Keszthelyi, L., Mouginiis-Mark, P. J., Rowland, S. K., and J. A. Resing, 1998, "Calculation of Lava Effusion Rates from Landsat TM Data," *Bulletin of Volcanology*, 60(1):52–71.

- Ingebritsen S. E., and S.A. Rojstaczer, 1996, "Geyser Periodicity and Response of Geysers to Deformation," *Journal of Geophysical Research*, 101(B10):21,891–21,905.
- Heasler, H., Jaworowski, C., and D. Susong, 2004, *A Geothermal Monitoring Plan for Yellowstone National Park*, Yellowstone National Park, WY: Yellowstone Center for Resources, 24 pp.
- Hurwitz, S., Jumar, A., Taylor, R., and H. Heasler, 2008, "Climate-Induced Variations of Geyser Periodicity in Yellowstone, National Park, USA," *Geological Society of America Bulletin*, 36(6):451–454.
- Husen, S., Taylor, R., Smith, R. B., and H. Heasler, 2004, "Changes in Geyser Eruption Behavior and Remotely Triggered Seismicity in Yellowstone National Park Produced by the 2002 M 7.9 Denali Fault Earthquake, Alaska," *Geology*, 32(6):537–540.
- Kennedy, R. E., Cohen, W. B., and T. A. Schroeder, 2007, "Trajectory-Based Change Detection for Automated Characterization of Forest Disturbance Dynamics," *Remote Sensing of Environment*, 110(3):370–386.
- Langford, N. P., 1972. *The Discovery of Yellowstone Park: Journal of the Washburn Expedition to the Yellowstone and Firehole Rivers in the Year 1870*, Lincoln, NE: University of Nebraska Press, 125 pp.
- Lawrence, R. L. and W. J. Ripple, 1999, "Calculating Change Curves for Multitemporal Satellite Imagery: Mount St. Helens 1980–1995," *Remote Sensing of Environment*, 67(3):309–319.
- Lu, D., Mausel, P., Brondizio, E., and E. Moran, 2003, "Change Detection Techniques," *International Journal of Remote Sensing*, 25(12):2365–2407.
- Morgan, L. A., Shanks, W. C., III, Loyalvo, D. A., Johnson, S. Y., Stephenson, W. J., Pierce, K. L., Harlan, S. S., Finn, C. A., Lee, G., Webring, M., Schulze, B., Duhn, J., Sweeney, R., and L. Balistrieri, 2003, "Exploration and Discovery in Yellowstone Lake: Results from High-Resolution Sonar Imaging, Seismic Reflection Profiling, and Submersible Studies," *Journal of Volcanology and Geothermal Research*, 122(3–4):221–242.
- Morgan, L. A., Shanks, W. C., Pierce, K. L., Loyalvo, D. A., Lee, G. K. Webring, M. W., Stephenson, W. J., Johnson, S. Y. Harlan, S. S., Schulze, B., and C. A. Finn, 2007, "The Floor of Yellowstone Lake Is Anything but Quiet—New Discoveries from High-Resolution Sonar Imaging, Seismic-Reflection Profiling and Submersible Studies," in *Integrated Geosciences Studies in the Greater Yellowstone Area—Volcanic, Tectonic, and Hydrothermal Processes in the Yellowstone Geocosystem*, Morgan, L. A. (Ed.), Reston, VA: U.S. Geological Survey Professional Paper 1717, 95–123.
- Muffler, L. J. P., White, D. E., and A. H. Truesdell, 1971, "Hydrothermal Explosion Craters in Yellowstone National Park," *Geological Society of America Bulletin*, 82(3):723–740.
- Neale, C., 2008, Personal Communication—Airborne Remote Sensing of Geothermal Heat Flux in Upper Geyser Basin in Yellowstone National Park, Missoula, MT.
- Nordstrom, D. K., McCleskey, R. B., and J. W. Ball, 2009, "Sulfur Geochemistry of Hydrothermal Waters in Yellowstone National Park: IV. Acid-Sulfate Waters," *Applied Geochemistry*, 24(2):191–207.

- Norton, D. R. and I. Friedman, 1985, "Chloride Flux Out of Yellowstone National Park," *Journal of Volcanology and Geothermal Research*, 26(3-4):231-250.
- NRCS (Natural Resource Conservation Service), 2009, "SNOTEL Data & Products" [<http://www.wcc.nrcs.usda.gov/snow/>], last accessed on February 22, 2009.
- Oechel, W. C., Vourlitis, G. L., Hastings, S. J., and S.A. Bochkarev, 1995, "Change in Arctic CO₂ Flux over Two Decades: Effects of Climate Change at Barrow, Alaska," *Ecological Applications*, 5(3):846-855.
- Oppenheimer, C., Rothery, D. A., and P. W. Francis, 1993, "Thermal Distributions at Fumarole Fields: Implications for Infrared Remote Sensing of Active Volcanoes," *Journal of Volcanology and Geothermal Research*, 55(1-2):97-115.
- Pierce, K. L. and L. A. Morgan, 1992, "The Track of the Yellowstone Hot Spot: Volcanism, Faulting, and Uplift," in *Regional Geology of Eastern Idaho and Western Wyoming*, Link, K., Kuntz, M. A., and L. B. Platt (Eds.), Boulder, CO: Geological Society of America, 53 pp.
- Pierce, K. L., Cannon, K. P., Meyer, G. A., Trebesch, M. J., and R. D. Watts, 2007, "Postglacial Inflation-Deflation Cycles, Tilting, and Faulting in the Yellowstone Caldera Based on Yellowstone Lake Shorelines," in *U.S. Geological Survey Professional Paper 1717*, 128-168.
- Roeloffs, E. A., 1988, "Hydrologic Precursors to Earthquakes: A Review," *Pageoph (Pure and Applied Geophysics)*, 126(2-4):134-139.
- Rojstaczer, S., Galloway, D. L., Ingebritsen, S. E., and D. M. Rubin, 2003, "Variability in Geyser Eruptive Timing and Its Causes: Yellowstone National Park," *Geophysical Research Letters*, 30(18):2-1-2-4.
- Rojstaczer, S. and S. Wolf, 1992, "Permeability Changes Associated with Large Earthquakes: An Example from Loma Prieta, California," *Geology*, 20(3):211-214.
- Rojstaczer, S., Wolf, S., and R. Michel, 1995, "Permeability Enhancement in the Shallow Crust as a Cause of Earthquake-Induced Hydrological Changes," *Nature*, 373(6511):237-239.
- Savage, S., Lawrence, R., Custer, S., Jewett, J., Powell, S., and J. Shaw, 2010, "Review of Alternative Methods for Estimating Terrestrial Emittance and Geothermal Heat Flux for Yellowstone National Park Using Landsat Imagery," *GIScience and Remote Sensing*, 47(4):460-479.
- Seielstad, C. and L. Queen, 2009, *Thermal Remote Monitoring of the Norris Geyser Basin, Yellowstone National Park. Final Report for the National Park Service Cooperative Ecosystem Studies Unit, Agreement No. H1200040001*, Missoula, MT: University of Montana, 38 pp.
- Smith, R. B. and L. J. Siegel, 2000, *Windows into the Earth—The Geologic Story of Yellowstone and Grand Teton National Parks*, New York, NY: Oxford University Press, 242 p.
- Sorey, M. L., 1991, *Effects of Potential Geothermal Development in the Corwin Springs Known Geothermal Resources Area, Montana, on the Thermal Features of Yellowstone National Park*, Menlo Park, CA: U.S. Geological Survey, Water-Resources Investigations Report 91-4052, 204 pp.
- Spatial Analysis Center, 1998, *30-Meter Elevation Data for Yellowstone National Park, Wyoming, Montana, Idaho*, Yellowstone National Park, WY: Yellowstone Center for Resources.

- Spatial Analysis Center, 2000, *Precipitation in Yellowstone National Park, Wyoming, Montana, Idaho*, Yellowstone National Park, WY: Yellowstone Center for Resources.
- Spatial Analysis Center, 2005, *Hydrogeothermal Areas of Yellowstone National Park, Wyoming, Montana, Idaho*, Yellowstone National Park, WY: Yellowstone Center for Resources.
- Spatial Analysis Center, 2008, *Thermal Inventory Point Data for Yellowstone National Park, 1998–2008*, Yellowstone National Park, WY: Yellowstone Center for Resources.
- Spicak, A., 2000, "Earthquake Swarms and Accompanying Phenomena in Intraplate Regions: A Review," *Studia Geophysica et Geodaetica*, 44(2):89–106.
- Thompson, G. R. and J. Turk, 2005, *Earth Science and the Environment*, Belmont, CA: Brooks/Cole–Thomson Learning, 601 pp.
- University of Utah, 2009, "Yellowstone National Park Region Earthquake Listings" [<http://www.quake.utah.edu/EQCENTER/LISTINGS/OTHER/yellowregion.htm>], last accessed March 15, 2009.
- University of Utah, 2011, "Yellowstone Hotspot Overview" [<http://www.yellowstone-gis.utah.edu/research/hotspot.html>], last accessed June 2, 2011.
- USGS (U.S. Geological Survey), 2008, "National Hydrography Dataset" [<http://nhd.usgs.gov/>], last accessed August 13, 2008.
- USGS (U.S. Geological Survey), 2009a, "Magnitude/Intensity Comparison" [http://earthquake.usgs.gov/learning/topics/mag_vs_int.php], last accessed March 17, 2009.
- USGS (U.S. Geological Survey), 2009b, "What Are the Earthquake Magnitude Classes?" [<http://earthquake.usgs.gov/learning/faq.php?categoryID=2&faqID=24>], last accessed March 17, 2009.
- Utah State University, 2008, "Image Standardization: At-Sensor Reflectance and COST Correction" [<http://earth.gis.usu.edu/imagestd/>], last accessed on April 8, 2009.
- Waring, G. A., Blankenship, R. R., and R. Bentall, 1983, *Thermal Springs of the United States and Other Countries of the World—A Summary*, Reston, VA: U.S. Geological Survey, USGS Professional Paper 492, 401 pp.
- Watson, F. G. R., Lockwood, R. E., Newman, W. B., Anderson, T. N., and R. A. Garrott, 2008, "Development and Comparison of Landsat Radiometric and Snowpack Model Inversion Techniques for Estimating Geothermal Heat Flux," *Remote Sensing of Environment*, 112(2):471–481.
- Western Regional Climate Center, 2005, "Period of Record Monthly Climate Summary—Yellowstone Park, Wyoming (489905)" [<http://www.wrcc.dri.edu/cgi-bin/cliRECTM.pl?wyell>], last accessed April 6, 2009.
- White, D. E., Fournier, R. O., Muffler, L. J. P., and A. H. Truesdell, 1975, *Physical Result of Research Drilling in Thermal Areas of Yellowstone National Park, Wyoming*, Washington, DC: U.S. Geological Survey, Professional Paper 892, 70 pp.
- White, D. E., Hutchinson, R. A. and T. E. C. Keith, 1988, *The Geology and Remarkable Thermal Activity of Norris Geyser Basin*, Yellowstone National Park, WY: U.S. Geological Survey, Professional Paper 1456, 84 pp.